Structural Study on Polymorphism of Cis-Unsaturated Triacylglycerol: Triolein

Chikayo Akita,† Tatsuya Kawaguchi, and Fumitoshi Kaneko*

Department of Macromolecular Science, Faculty of Science, Osaka University, Toyonaka, Osaka 560-0043, Japan

Received: September 4, 2005; In Final Form: December 25, 2005

To clarify the influence of cis-unsaturation on solid-state structures of triacylglycerols (TAGs), the crystal structures of three crystalline phases (α, β' and β) of triolein [$C_3H_5(OCOC_{17}H_{33})_3$] were investigated by powder X-ray diffractometry and IR and Raman spectroscopy. The influence on the structural change of the α phase in the course of cooling was also studied. With respect to the subcell structure and conformational order of hydrocarbon chains in the β and β' phases, triolein resembles saturated TAGs; trans-zigzag hydrocarbon chains are adopted in the $T_{\parallel}$ subcell for the β phase and in the $O_{\perp}$ subcell for the β' phase. The influence of cis-unsaturation was most obvious in the structure of the α phase and its temperature dependence. The α phase of triolein does not form the ordinary hexagonal subcell but a rather loose distorted subcell, which hardly changes in cooling, forming a striking contrast to the hexagonal → pseudohexagonal subcell transformation found in the α phase of saturated TAGs.

Introduction

Triacylglycerols (TAGs) are the major constituents of fats and oils that form a large group of lipids. TAGs consist of a glycerol backbone and three esterified fatty acids. Many different kinds of fatty acids have been found in TAGs.[1] In particular, cis-unsaturated acyl chains are abundant in naturally occurring TAGs. For example, oleic acid (*cis*-9-octadecenoic acid) accounts for 85% of fatty acids in olive oil, and erucic acid (*cis*-13-docosenoic acid) accounts for one-half of fatty acids in indigenous-canola oil. According to studies on *cis*-unsaturated fatty acids, *cis*-unsaturation changes the overall configuration of acyl chains and their lateral packing in solid states, resulting in their characteristic properties such as reversible solid-state phase transitions.[2] However, the structure and physicochemical properties of cis-unsaturated TAGs in solid states have not been fully understood yet.

One of the important features of TAGs is polymorphism.[3,4] Depending on the crystallization conditions and thermal history, a variety of solid states of TAGs are generated. Because the solid-state properties depend remarkably on the polymorphic phases, the control of polymorphism is a very important subject in the industrial field. However, the polymorphism of cis-unsaturated TAGs is less understood than that of saturated TAGs.[5−8]

Triolein, $C_3H_5(OCOC_{17}H_{33})_3$, where three oleic acid molecules are linked to a glycerol group, is a main constituent of olive oil. The existence of three polymorphic phases of triolein, β, β' and α, was confirmed by Lutton et al.[9] and Wheeler et al.[10] on the basis of X-ray diffraction and thermal data as shown in Figure 1. Later on, Hagemann et al.[11] reported that at least three kinds of the β' phases ($\beta'1$, $\beta'2$ and $\beta'3$) appeared depending on crystallization conditions.

However, little is known about the molecular conformation and packing in these solid phases, which would be ascribed to the following two things. First, the preparation of single specimens suitable for X-ray structural analysis is very difficult even for the stable β phase. Second, the other metastable phases intrinsically contain a lot of disorders, and therefore, only limited structural information can be obtained from several diffused X-ray reflections.

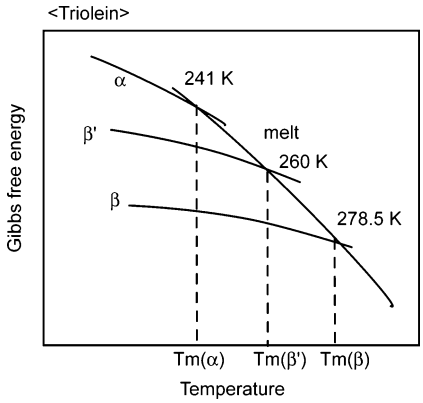

Figure 1. Relationship between Gibbs free energy and temperature for three modifications of triolein.[9,10]

In this study, we conducted a structural study on triolein with a combination of powder X-ray diffraction method and vibrational spectroscopy (IR and Raman). The latter is able to deduce the structural information about local functional groups even from a powdery sample. We investigated the conformation of *cis*-olefin group and conformational order and subcell structure of hydrocarbon chains in each polymorphic phase, especially in the β and α phases.

Another aim of this paper is to clarify the influence of cis-unsaturation on the structural change of the α phase on the course of cooling. As for saturated TAGs, a large structural change takes place in the α phase, whose acyl chains are packed most loosely among the solid phases of TAGs; the lateral packing mode of acyl chains changes from the hexagonal (H) subcell structure to the pseudohexagonal (p-H) one.[12,13] Our previous studies indicated that *cis*-olefin groups greatly change

* Corresponding author. (Phone) +81-6-6850-5453. (Fax) +81-6-6850-5288. E-mail: toshi@chem.sci.osaka-u.ac.jp.

† Present address: Nitto Analytical Techno-Center Co., Ltd. 1-1-2, Shimohozumi, Ibaraki, Osaka 567-8680, Japan. E-mail: chikayo_takechi@gg.nitto.co.jp.

10.1021/jp054996h CCC: $33.50
Published on Web 02/04/2006

the lateral packing of hydrocarbon chains of cis-unsaturated fatty acids.[14−17] It seems reasonable to suppose that *cis*-olefin groups affect significantly the structural changes of the α phase induced by cooling. To confirm this expectation, we investigated the dependence of lateral packing of acyl chains on temperature for the α phase of triolein.

Experiment Section

Sample. A sample of triolein (>99% purity) was purchased from Sigma Co. Ltd. For powder X-ray diffraction and Raman measurements, a sample of the α phase was prepared by cooling a melt to 93 K at a rate of about 10 °C/min. Samples of the β and β' phases were obtained by cooling a melt to 233 K at a rate of about 10 °C/min, holding for 5 min, and then heating and holding at 273 and 245 K, respectively.[9] For IR measurements, a sample of each polymorph was obtained by conducting the same cooling treatment on a melt sample sandwiched between a couple of KBr windows.

Measurements. Powder X-ray diffraction diagrams were taken by using a RIGAKU RINT 2000 diffractometer with Cu Kα radiation (40 kV and 40 mA), equipped with liquid N_2 flow type cryostat for low-temperature measurement. The data were collected over a 2θ range from 2 to 70° at 0.5°/min with a step size of 0.05°. IR spectra were taken with a JASCO FT-IR 8300 spectrometer. The resolution and number of scans were set at 2 cm^{-1} and 64, respectively. Raman spectra were measured with a JASCO NR-1800 double monochromator using 514.5 nm line (Ar^+ laser) as the excitation source. For measurements of IR and Raman spectra at low temperatures, an Oxford continuous flow type was employed.

Background

A. Simple Coupled Oscillators Model for Long Chain Compounds. Vibrational spectra of long-chain molecules have been interpreted on the basis of the vibrational modes of an infinite polymethylene chain,[18−21] whose frequencies change as functions of the phase angle ϕ: the difference in phase between neighboring methylene units. As for an infinite extended chain, only the vibrational modes of $\phi = 0$ or π can be observed in IR and Raman spectra. On the contrary, a finite extended chain shows a series of bands called progression bands in IR and Raman spectra, each of which corresponds to an intermediate phase angle.

The allowed phase angles for a finite chain can be estimated with the simple coupled oscillators model where each oscillator interacts only with nearest neighbor oscillators. Here, we consider the following two extreme conditions for a system composed of n oscillators at positions 1 to n and two end groups at position 0 and $n + 1$: fixed−fixed boundary condition, where the displacements of the two ends, A_0 and A_{n+1} are both zero, and fixed−free boundary condition,[22] where A_0 equals zero and A_{n+1} is at the maximum.

A standing wave of a simple coupled oscillator has a form

$$A_i = B \sin \phi \cdot i \tag{1}$$

for both the fixed−fixed boundary and the fixed−free boundary models from the condition of $A_0 = 0$, where A_i is the displacement of an oscillator at position i and B is a constant.

When the condition of another end for the fixed−fixed boundary, $A_{n+1} = 0$, is applied to eq 1, we obtain $(n + 1)\phi = k\pi$, where k is an integer. Therefore, the allowed phase angles are given as

$$\phi = k\pi/(n + 1) \qquad k = 1, 2, 3, ..., n \tag{2}$$

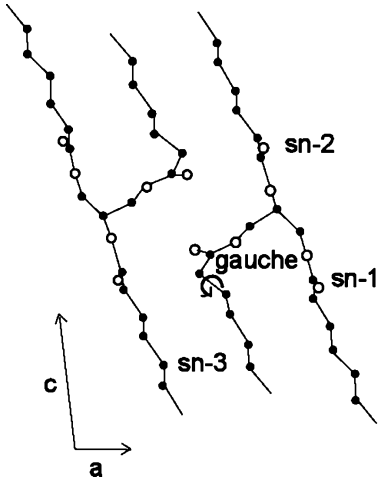

Figure 2. Molecular packing in the vicinity of the glycerol backbone in the β phase of saturated TAGs, which is created from the coordinate data taken from refs 5 and 6.

Similarly, using the condition of $A_{n+1} = \pm B$ for the fixed−free boundary, we obtain $\phi(n + 1) = (2k - 1)\pi/2$. The allowed phase angles are given as

$$\phi = [(2k - 1)\pi]/2(n + 1) \qquad k = 1, 2, 3, ..., n \tag{3}$$

B. Vibrational Modes of the Oleoyl Chain. An oleoyl chain linked to the glycerol backbone of TAGs can be divided into two portions by *cis*-C═C bond; glycerol-sided chain and methyl-sided one. The former can be regarded as a finite chain with a fixed−fixed boundary and the latter as one with a fixed−free boundary. Both chains consist of seven methylene groups. Applying eqs 2 and 3, we obtain the allowed phase angles

$$\phi = (2k - 1)\pi/16 \qquad k = 1, 2, 3, ..., 7 \tag{4}$$

for the straight methyl-sided chain, and

$$\phi = k\pi/8 \qquad k = 1, 2, 3, ..., 7 \tag{5}$$

for the straight glycerol-sided chain.

In case that an acyl chain takes a gauche conformation in the vicinity of the glycerol backbone just like the sn-3 chain in the β phase of saturated monoacid TAGs as shown in Figure 2, the number of coupled oscillators is reduced by one.[23] Therefore, the allowed phase angles for the bent glycerol-sided chain are obtained by assuming a value of $n = 6$ into eq 2,

$$\phi = k\pi/7 \qquad k = 1, 2, 3, ..., 6 \tag{6}$$

Results and Discussion

***β* phase.** *A. Molecular Structure.* The conformation of the glycerol backbone is an important factor to determine the overall molecular configuration of TAGs. As for saturated monoacid TAGs, the β phase consists of two straight chains linked at the sn-1 and 2 positions and a bent chain linked at the sn-3 position which has a gauche bond in the vicinity of the ester group bound to the glycerol. In such a configuration of the glycerol, the sn-1 and 3 chains are adjacent, and the sn-2 chain forms the back rest of the chair. Here, we call this configuration the "sn-1,3 chair configuration" after Birker et al.,[24] which corresponds to the [$\alpha p/\gamma\beta$/sc] conformer in the nomenclature of Pascher et al.[25] This configuration has been confirmed also in the β phase of a trans-unsaturated TAG, trielaidin.[26,27] The following spectral data suggest that the β phase of triolein also has the sn-1,3 chair configuration.

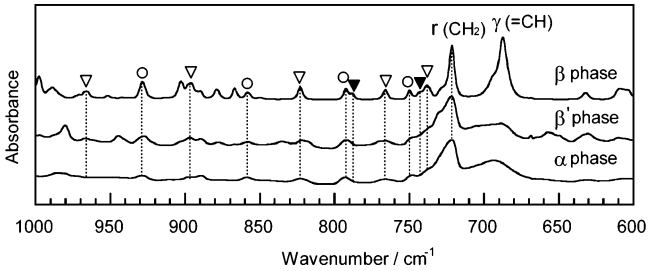

Figure 3. IR spectra in the CH_2 rocking region of the β phase at 70 K, the β' phase at 70 K and the α phase at 93 K. The bands marked with open circles, open wedges and closed wedges indicate the ν_8 progression bands of the methyl-sided chain, the glycerol-sided straight chain and the glycerol-sided bent chain, respectively.

TABLE 1: Frequencies and Assignments of IR Bands in the CH_2 Rocking Region of Triolein

β frequency (cm^{-1})	α frequency (cm^{-1})	assignment[a]
720	722	R1-t (C═O side)
735	735	R3-t (C═O side)
743		R3-g (C═O side)
750	749	R4 (CH_3 side)
766	766	R4-t (C═O side)
790		R4-g (C═O side)
794	794	R5 (CH_3 side)
823	822	R5-t (C═O side)
859	859	R6 (CH_3 side)
898	898	R6-t (C═O side)
929	929	R6 (CH_3 side)
963		R7-t (C═O side)

[a] R: ν_8 mode. t: straight chain. g: bent chain.

(1) Progression Bands in IR CH_2 Rocking Region. Figure 3 shows the representative IR spectra in the CH_2 rocking region. Most bands appearing in this region can be assigned to the progression bands due to the CH_2 rocking-twisting (ν_8) branch modes of hydrocarbon segments. The ν_8 progression bands are highly sensitive to the length and conformational state of a hydrocarbon chain, because the phase-angle dependence of the ν_8 branch is so strong that a structural change of a hydrocarbon chain causes definite frequency shifts of the progression bands.

The spectrum of β phase of triolein in this region is very complicated, which can be ascribed to two factors. One is the division of oleoyl group into two chains by a *cis*-C═C bond, and the other is the bent conformation of oleoyl group in the vicinity of the glycerol backbone. The two chains, i.e., the methyl-sided and glycerol-sided chains, both consist of the seven methylene groups. However, even when they both take the all-trans conformation, the allowed phase angles of vibrational modes are different between them as shown in eqs 4 and 5 due to the difference in the boundary conditions. The bands with open circles in Figure 3 can be assigned to the ν_8 progression modes of the methyl-sided straight chain, and the bands with open wedges to those of the glycerol-sided chain. Meanwhile, the bands with closed wedges can be allocated to the ν_8 modes of the bent glycerol-sided chain given by eq 6. The assignments of these bands are summarized in Table 1. Figure 4 shows the frequency vs phase angle plot with the observed frequencies and the phase angles obtained from eqs 4−6. This plot well represents the features of ν_8 branch,[18,20] suggesting the validity of the assignments.

From the analysis described above, it is suggested that all three methyl-sided chains and two glycerol-sided chains take all-trans conformation whereas one glycerol-sided chain has a gauche conformation at the neck.

(2) Progression Bands in IR CH_2 Wagging Region. Figure 5 shows IR spectra in the 1500−1100 cm^{-1} region, in which the

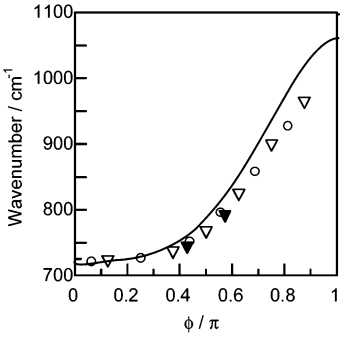

Figure 4. Frequency-phase difference curve for the ν_8 branch mode and observed frequency data of the methyl-sided chain (open circles), the glycerol-sided straight chain (open wedges) and the glycerol-sided bent chain (closed wedges). The solid line indicates the calculated dispersion curve for an infinitely long polymethylene chain.[18,20]

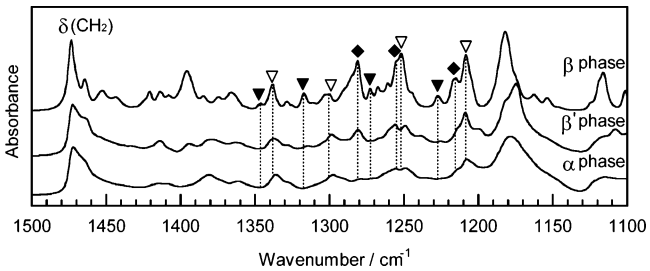

Figure 5. IR spectrum in the CH_2 wagging region of the β phase at 70 K, the β' phase at 70 K and the α phase at 93 K. The bands marked with open wedges and closed wedges indicate the ν_3 progression bands of the glycerol-sided straight chain and those of the glycerol-sided bent chain, respectively. The bands marked with closed diamonds indicate the ν_7 progression bands of the glycerol-sided bent chain.

progression bands due to both the ν_7 (CH_2 twisting − rocking) and ν_3 (CH_2 wagging) modes appear.

The bands due to the ν_7 and ν_3 modes are originally weak, and gain appreciable intensity through the coupling with the C−O stretch mode of the ester group bound to the glycerol backbone.[21,28] Therefore, it seems reasonable to assume that the modes due to the glycerol-sided chains mainly contribute to this region. In addition, the intensity of the ν_7 mode depends on the conformation of the acyl chain in the vicinity of the ester bond:[29,30] the ν_7 progression bands become intense when the acyl chain takes the bent conformation.[23]

From the above discussion, we can expect that three series of the progression bands make dominant features in case that triolein takes the chair configuration: the ν_3 progression bands of the straight chain, and the ν_3 and ν_7 ones of the bent chain, which well agrees with the observed spectra. The bands marked with open wedges and closed wedges in Figure 5 can be assigned to the ν_3 modes of the phase angles obtained from eqs 5 and 6 for the straight and bent glycerol-sided chains. The bands with closed diamonds are due to the ν_7 mode of the phase angles obtained from eq 6. These assignments are listed in Table 2. The frequency vs phase angle plots shown in Figures 6 and 7 coincide with the ν_3 and ν_7 dispersion curves, which bears out this analysis.

(3) Carbonyl Stretch Bands in IR and Raman Spectra. It has been shown that the conformation around the glycerol group is also reflected in the IR and Raman bands due to the carbonyl stretch mode [ν(C═O)]. In the β phase of tripalmitin and trielaidin,[27,31] for example, the ν(C═O) band due to the straight sn-1 and 2 chains and that due to the bent sn-3 chain appear at 1738 and 1728 cm^{-1}, respectively.

The β phase of triolein exhibits similar spectral features. The IR ν(C═O) band splits into two bands at 1738 and 1729 cm^{-1}

TABLE 2: Frequencies and Assignments of IR Bands in the CH_2 Wagging Region of Triolein

β frequency (cm^{-1})	α frequency (cm^{-1})	assignment[a]
1208	1208	W1-t (C═O side)
1215	1215 (shoulder)	T1-g (C═O side)
1226		W1-g (C═O side)
1252	1250	W2-t (C═O side)
1254	1254	T2-g (C═O side)
1272		W2-g (C═O side)
1280		T3-g (C═O side)
1299	1298	W3-t (C═O side)
1316		W3-g (C═O side)
1339	1337	W4-t (C═O side)
1346		W4-g (C═O side)

[a] W: ν_3 mode. T: ν_7 mode. t: straight chain. g: bent chain.

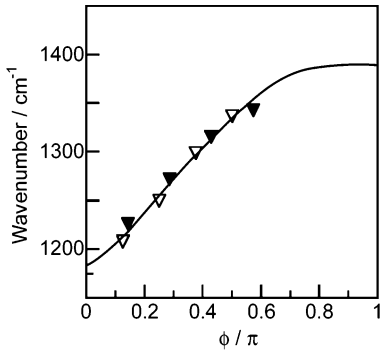

Figure 6. Frequency-phase difference curve for the ν_3 branch mode and observed frequency data of the glycerol-sided straight chain (open wedges) and the glycerol-sided bent chain (closed wedges). The solid line indicates the calculated dispersion curve for an infinitely long polymethylene chain.[18,20]

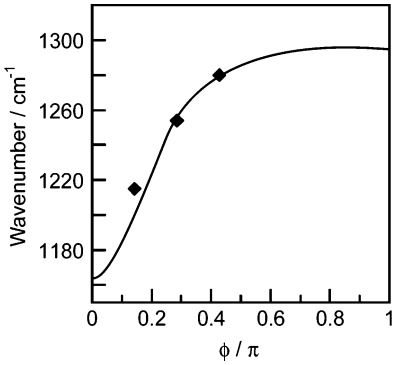

Figure 7. Frequency-phase difference curves for the ν_7 branch mode with observed frequency data of the glycerol-sided bent chain. The solid line indicates the calculated dispersion curve for an infinitely long polymethylene chain.[18,20]

and Raman band splits into two bands at 1744 and 1728 cm^{-1} as shown in Figure 8a,b.

As described above, the coexistence of the straight and bent glycerol-sided chains in triolein β phase are suggested by vibrational spectral data, from which we speculate that the β phase of triolein takes the sn-1,3 chair configuration having two straight chains at the sn-1 and 2 positions and a bent chain at the sn-3 position.

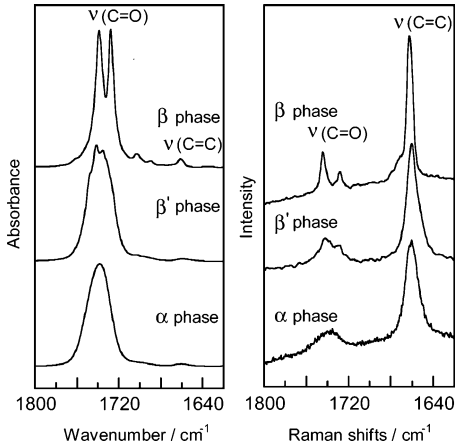

Figure 8. IR (a) and Raman (b) spectra in the C═O stretch region of the β phase at 70 K, the β' phase at 70 K and the α phase at 93 K.

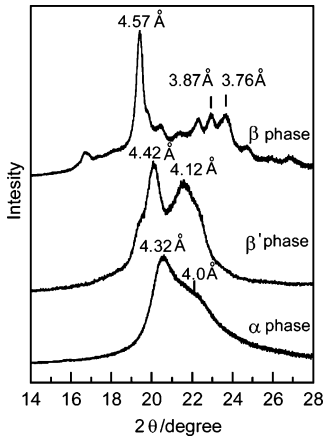

Figure 9. XRD diagrams of the β phase at 273 K, β' phase at 245 K and α phase at 193 K.

B. Conformation of the cis-Olefin Group. As the conformation of *cis*-olefin group determines the overall shape of acyl chains, it has a strong influence on the lateral packing and dynamic properties of cis-unsaturated acyl chains. So far, a variety of conformations have been found. The frequencies of vibrational modes due to the *cis*-olefin group depend sensitively on its conformation. Some examples of cis-monounsaturated fatty acids are listed in Table 3.[15] The Raman C═C stretch ν(C═C) band and the IR ═C−H out of plane bend γ(═CH) band are good indicators for the conformation of the *cis*-olefin group. The frequencies of the ν(C═C) and γ(═CH) bands of triolein β phase are similar to those of oleic acid γ, as listed in Tables 3 and 4. These data suggest that the *cis*-olefin groups of triolein β take the skew−cis−skew′ conformation.

C. Subcell Structure. The X-ray diffraction (XRD) pattern in the region of $d = 3.0-6.0$ Å reflects sensitively the lateral packing of hydrocarbon chains. The β phases of saturated and trans-unsaturated TAGs take the $T_{||}$ subcell. As shown in XRD patterns of Figure 9, triolein β exhibits three intense reflections of 4.57, 3.87 and 3.76 Å spacings characteristic of the $T_{||}$ subcell, which is consistent with the previous X-ray study done by Lutton et al.[9]

TABLE 3: IR and Raman Bands Associated with the Olefin Conformation of Unsaturated Fatty Acids (Frequencies in cm^{-1})

	skew−cis−trans oleic acid α		skew−cis−skew′ oleic acid γ		trans−cis−trans oleic acid β	
assignment	Raman	IR	Raman	IR	Raman	IR
C═C stretch	1657	1664	1661	1664	1642	1645
═C−H out of plane bend		695		704		645

TABLE 4: IR and Raman Bands Associated with the Olefin Group of Triolein (Frequencies in cm^{-1})

	β phase		β' phase		α phase	
assignment	Raman	IR	Raman	IR	Raman	IR
C═C stretch	1662	1661	1660	1660	1661	1660
═C−H out of plane bend		687				692

The $T_{||}$ subcell of triolein β is also suggested by IR spectral data. The CH_2 rocking [r(CH_2)] and scissoring [δ(CH_2)] modes sensitive to subcell structure were observed as intense singlet bands at 720 and 1471 cm^{-1}, respectively, as shown in Figures 3 and 5. These singlet bands are the characteristic of the $T_{||}$ subcell structure. Therefore, it can be inferred that both the methyl-sided and the glycerol-sided hydrocarbon chains form the $T_{||}$ subcell structure.

Our conclusion is that the β phase of triolein has the characteristics common to the β phase of saturated TAGs. Namely, the unit cell of space group $P\bar{1}$ consists of two triolein molecules taking the sn-1,3 chair configuration, and the methyl-sided and glycerol-sided chains bounded to the *cis*-C═C group of skew−cis−skew′ conformation are adopted in the $T_{||}$ subcell.

α phase. *A. Molecular Structure.* Previous studies on saturated and trans-unsaturated TAGs showed that TAG molecules in the α phase do not take the sn-1,3 chair configuration; the glycerol backbone and its neighbor are conformationally disordered.[27,31] The following spectral data suggest that the α phase of triolein also has selective conformational disorders in the glycerol-sided chains.

(1) Progression Bands in IR CH_2 Rocking and Wagging Regions. As has been described, triolein β has three different kinds of hydrocarbon chains are contained in the β phase; two straight glycerol-sided chains, a bent glycerol-sided chain, and three straight methyl-sided chains.

As shown in Figure 3, only the bands due to the methyl-sided and straight glycerol-sided chains are observed in the α phase, but the bands due to the bent chain are absent. All bands become broadened, in particular, a marked broadening takes place at the glycerol-sided bands.

These spectral features imply that the absence of a definite bent structure and a decrease in conformational regularity for the glycerol-sided chains.

Similar spectral features are observed in the CH_2 wagging region as shown in Figure 5. Most ν_3 and ν_7 bands due to the bent glycerol-sided chain disappear in the α phase. The remaining ν_3 bands due to the straight glycerol-sided chains become broader than those of the β phase.

(2) Carbonyl Stretch Bands in IR and Raman Spectra. The α phase does not show such a clear splitting of IR ν(C═O) bands as observed in the β phase, as shown in Figure 8a. In the α phase, the band due to the bent glycerol-sided chain is absent, and only a broad band centered at 1739 cm^{-1} is observed. Similar characteristics are also observed in Raman spectra in Figure 8b.

(3) Raman Spectrum in the CC Stretch Region. The decrease in conformational regularity for the glycerol-sided chains is also confirmed with the Raman bands due to the CC stretch, which are highly sensitive to the conformational state of polymethylene chains. Oleic acid shows three intense bands in the CC stretch region when having an ordered structure: the symmetric CC stretch [ν_s(CC)] band of the methyl-sided chains at 1125 cm^{-1}, the ν_s(CC) band of the carboxyl-sided chains at 1095 cm^{-1}, and the antisymmetric CC stretch [ν_a(CC)] band due to both the methyl-sided and carboxyl-sided chains at 1063 cm^{-1}.[15] The frequency gap of about 30 cm^{-1} between the two ν_s(CC) bands

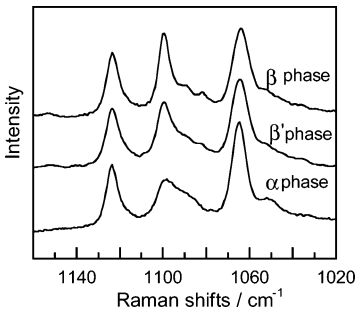

Figure 10. Raman spectra in the CC stretch region of the β phase at 273 K, the β' phase at 245 K and the α phase at 193 K.

is caused by the difference in the boundary conditions of hydrocarbon chains and the high-frequency dispersiveness of the CC stretch modes.

Similarly, triolein β shows the ν_s(CC) bands of the methyl-sided and glycerol-sided chains at 1124 and 1099 cm^{-1}, as shown in Figure 10. Using these two ν_s(CC) bands, the conformational states of the two hydrocarbon chains can be monitored separately. In the α phase, the intensity of the glycerol-sided ν_s(CC) band becomes weak and has a shoulder at the low-frequency side. Such a large difference is not observed for the methyl-sided ν_s(CC) band. From these results, we can say that the conformational regularity of the glycerol-sided chain is decreased compared with that of the methyl-sided chain in the α phase.

B. cis-Olefin Group. There is a marked similarity in the frequencies of the bands due to *cis*-olefin group between the α and β phases of triolein and the γ phase of oleic acid taking the skew−cis−skew′ conformation (Tables 3 and 4). However, these bands are rather broadened in the α phase, in particular, the IR ═C−H out of plane bend γ(═CH) band. These data seem to suggest that the conformation of *cis*-olefin group is distributed in a certain range centering around the exact skew−cis−skew′ conformation in the α phase.

C. Subcell Structure. Triolein shows a different feature in the XRD diagram of the α phase from saturated TAGs. Saturated TAGs show an intense reflection at 4.2 Å due to the hexagonal subcell (H), whereas triolein α shows a broad peak at 4.32 Å and a shoulder at 4.00 Å in XRD diagram (Figure 9) as Lutton et al. reported.[9] The single subcell reflection of the H subcell is due to the isotropic packing of hydrocarbon chains, and this feature of triolein means that the lateral packing is anisotropic, in other words, the packing density of hydrocarbon chains is directional dependent.

Such differences appear in IR measurement. The α phase of saturated TAGs shows relatively sharp singlet bands at 720 and 1468 cm^{-1} due to CH_2 rocking r(CH_2) and CH_2 scissoring δ-(CH_2) modes, respectively, which is the characteristics of the H subcell, whereas the triolein α phase shows asymmetric broadened bands at 722 and 1470 cm^{-1} due to r(CH_2) and δ-(CH_2) modes, respectively, as shown in Figures 3 and 5.

As have been discussed, triolein α keeps the conformational regularity of the methyl-sided chain. Even the glycerol-sided chains, which contain disorders to an extent, have such a level of regularity that the weak ν_3 and ν_7 progression bands appear. Therefore, the above characteristics observed in XRD and IR measurements cannot be attributed to a decrease in the conformational regularity. We view them more as an indication of a different lateral packing structure and infer that the α phase of triolein has a subcell structure distorted from the H subcell.

***β′* Phase.** *A. Molecular Structure.* The β' phase of saturated monoacid TAGs carries out a solid-state transition to the β

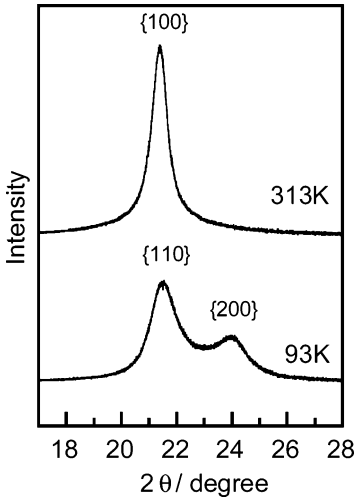

Figure 11. XRD diagrams of saturated TAG, tristearin, in the α phase at 313 K and the sub-α phase at 93 K.

phase, based on which Larsson et al. inferred that the glycerol group of the β' phase takes a similar configuration to that of β phase, i.e., the sn-1,3 chair configuration.[32] Yano et al. arrived at the same conclusion from the results of IR spectroscopic experiments.[33] As described below, our vibrational spectroscopic data suggest that the β' phase of triolein also has the sn-1,3 chair configuration, as does the β phase but is conformationally less ordered than the β phase as to glycerol and glycerol-sided chain and *cis*-olefin group.

In the CH_2 wagging region, the β' phase shows more peaks than the α phase, as shown in Figure 5. In addition to the ν_3 bands due to the straight glycerol-sided chain, a few bands due to the bent glycerol-sided chain are also observed. In particular, the ν_7 band at 1280 cm^{-1} appears clearly.

In the CH_2 rocking region, the ν_8 progression bands due to the bent and straight glycerol-sided chains are observed as shown in Figure 3. Although these progression bands are rather broad compared with those in the β phase, their appearance suggests that the glycerol-sided chains become more ordered than those in the α phase. The following are consistent with the characteristics of these progression bands. In the Raman CC stretching region (Figure 10), the ν_s (CC) band of the glycerol-sided chain is more intense and sharper than that of the α phase, indicating higher conformational regularity. The IR C═O stretch band shows a shoulder at 1730 cm^{-1} and Raman band shows two maximum at 1741 and 1730 cm^{-1} as observed in the β phase (Figure 8), suggesting the bent conformation.

As for the subcell structure, there are many pieces of evidence for the $O_\perp$ subcell. In IR spectra, the CH_2 rocking band splits into a doublet at 722 and 730 cm^{-1} and the CH_2 scissoring band also splits into a doublet at 1472 and 1465 cm^{-1} as shown in Figures 3 and 5. These are the typical characteristics of the $O_\perp$ subcell. In the XRD diagram, two peaks due to {110} and {200} reflections of the $O_\perp$ subcell appear at 4.42 and 4.12 Å (Figure 9).

Temperature Dependence of the α Phase

Jackson et al. and Goto et al. reported that the α phase of saturated TAG such as tristearin gradually transforms to the sub-α phase having the pseudohexagonal (p-H) subcell on cooling.[12,13] As shown in Figure 11, the reflection at 4.15 Å due to the {100} plane of the H subcell splits into the doublet at 4.14 and 3.72 Å due to the {110} and {200} planes of the p−H subcell in the sub-α phase.

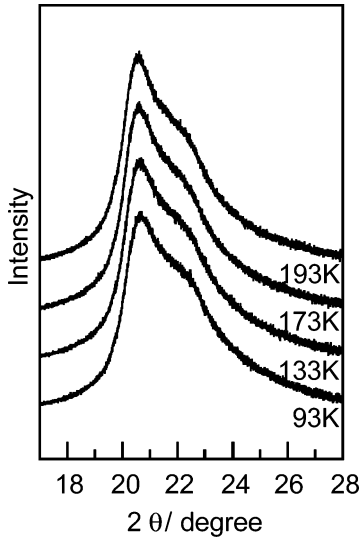

Figure 12. Temperature dependence of the XRD diagrams in the α phase.

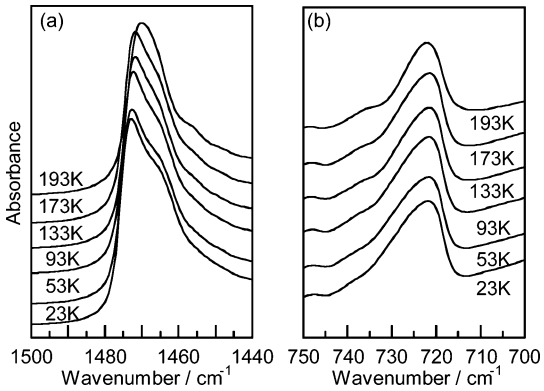

Figure 13. Temperature dependence of the IR spectra in the α phase in the CH_2 scissoring (a) and CH_2 rocking regions (b).

On the contrary, the XRD diagram of triolein α hardly changes in the course of cooling (Figure 12).

The CH_2 scissoring $\delta(CH_2)$ and CH_2 rocking $r(CH_2)$ bands sensitive to the subcell structure also showed no marked spectral change (Figure 13). These results suggest that no substantial change takes place in the lateral packing of polymethylene chains of triolein α on the course of cooling. The Raman CC stretch region ν_s(CC) in Figure 14 also shows no striking spectral change, indicating that the conformational regularity of hydrocarbon chain remains unchanged on cooling.

On the course of heating, triolein α gradually transforms to the β phase. The broadened CH_2 rocking band at 722 cm^{-1} becomes a sharp singlet band at 720 cm^{-1}, and the reflection 4.57 Å spacing (at 19.42°) increases with temperature. These features of the β phase start to appear around 213 K.

Influence of the *cis*-C═C Bond on Polymorphism of TAGs

As described above, the β and β' phases of triolein have structural features common to saturated TAGs with respect to molecular conformation and subcell structure: the sn-1,3 chair configuration and the $T_{||}$ and $O_\perp$ subcells in the β and β' phases.[5−8,32,33] On the contrary, the α phase of triolein is significantly different from the α phase of saturated TAGs: a loose subcell structure distorted from the H subcell and a largely disordered glycerol-sided hydrocarbon chains. The latter point is a uniqueness of unsaturated TAGs. Usually, long-chain

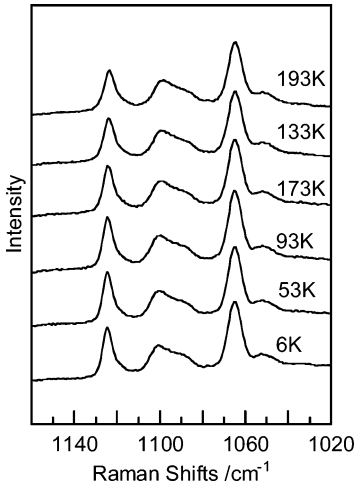

Figure 14. Temperature dependence of the Raman spectra in the CC stretch region in the α phase.

compounds tend to have conformational disordering at their methyl ends. For instance, on the reversible solid-state phase transitions of cis-monounsaturated fatty acids, the conformational disordering takes place only in the methyl-sided chains.[15] The fact that the glycerol-sided chain is more disordered than the methyl-sided one in the α phase makes a sharp contrast with this tendency of cis-monounsaturated fatty acids.

We presume that the difference in crystallization conditions brings about a striking difference in the influence of cis-unsaturation on crystal structure. The stable phase β crystallizes in the highest temperature region among the three solid phases, and therefore, its growth rate is low under such a low supercooling condition. It is reasonable to suppose that triolein molecules attached on the growth front of a growing crystal have a plenty of time for finding a stable position and adjusting the molecular conformation before the next molecular layer is formed over them. The situation would lead the molecules to take an ordered $T_{\parallel}$ subcell and the sn-1,3 chair configuration regardless of the steric hindrance of *cis*-olefin groups. As for the β' phase that crystallizes in the next lower temperature region, a similar situation would develop on the crystallization of the β' phase.

In contrast, the α phase grows rapidly at large supercoolings. Such a rapid crystallization often brings about several metastable states containing several kinds of disorders. In the crystallization of triolein α, molecules are strongly urged to solidify and do not have enough time to form the stable molecular packing and conformation. In this case, the restriction of *cis*-olefin group on triolein molecules should have a strong effect on the lateral packing of acyl chains. The bent configuration at *cis*-C═C bond prevents the acyl chains from forming the H subcell and leads them to a rather loose anisotropic lateral packing. Furthermore, the steric hindrance of *cis*-olefin group would hinder the contraction of subcell in the lateral direction by cooling.

We would speculate that the difference in terminal condition between the methyl-sided and glycerol-sided chain strongly affects the mobility of these parts, and the difference in mobility is the cause of the conformational disorder concentrated in the glycerol-sided chain. No sooner is a molecule incorporated into the growth front of a crystalline phase than its rearrangement into a stable structure starts. The methyl-sided chain having a free end is able to rearrange its position readily in the rapid crystallization of the α phase. On the contrary, the rearrangement of the glycerol-sided chain is strongly depressed, because the motion of this portion is highly restricted by the glycerol group and the *cis*-C═C bond. It follows that the relaxation to the stable molecular conformation and packing requires much longer time for the glycerol-sided chains than for the methyl-sided chains. Therefore, it is reasonable to suppose that the glycerol-sided chain loses its mobility before its rearrangement is completed and some conformational disorders are left in this portion.

Conclusion

The crystal structures of the α, β' and β phases of triolein $[C_3H_5(OCOC_{17}H_{33})_3]$ and the structural change of the α phase by cooling were investigated by X-ray diffraction and IR and Raman spectroscopies, through which the following results were obtained.

(1) The β and β' phases of triolein have characteristics common to those of saturated TAGs; the acyl chains form the $T_{\parallel}$ and $O_{\perp}$ subcell structures with conformationally ordered acyl chains. (2) The α phase of triolein has a rather unique structure. It does not form the H subcell characteristic of the α phase of saturated TAGs but a loose subcell structure whose packing density has a directional dependence. The glycerol-sided chain has an appreciable amount of conformational disorders. (3) In the cooling process of the α phase, triolein hardly shows such a structure change as the H → p-H subcell transformation found in saturated TAGs.

These results mean that the influence of cis-unsaturation is reflected most in the structure of the metastable α phase, which can be understood from the viewpoint of the structure formation in a rapid crystallization.

References and Notes

(1) Pryde, E. H. *Fatty acids*; The American Oil Chemists' Society: Champaign, Illinois, 1979.
(2) Kaneko, F.; Yano, J.; Sato, K. *Curr. Opin. Struct. Biol.* **1998**, *8*, 328.
(3) Garti, N.; Sato, K. *Crystallization and Polymorphism of fats and Fatty acids*; Marcel Dekker: New York, 1995.
(4) Small, D. M. *The physical Chemistry of Lipids*; Plenum: New York, 1986.
(5) Jensen, L. H.; Mabis, A. J. *Acta Crystallogr.* **1966**, *21*, 770.
(6) Larsson, K. *Ark. Kemi.* **1964**, *23*, 1.
(7) Larsson, K. *Proc. Chem. Soc.* **1963**, 87.
(8) Mykhaylyk, O. O.; Hamley, I. W. *J. Phys. Chem. B* **2004**, *108*, 8069.
(9) Ferguson, R. H.; Lutton, E. S. *J. Am. Chem. Soc.* **1947**, *69*, 1445.
(10) Wheeler, D. H.; Riemenschneider, R. W.; Sando, C. E. *J. Biol. Chem.* **1940**, *132*, 687.
(11) Hagemann, J. W.; Tallent, W. H.; Kolb, K. E. *J. Am. Oil Chem.* **1986**, *90*, 6371.
(12) Jackson, F. L.; Lutton, E. S. *J. Am. Chem. Soc.* **1950**, *72*, 4519.
(13) Goto, M.; Asada, E. *Yukagaku* **1967**, *16*, 402.
(14) Kaneko, F.; Yamazaki, K.; Kobayashi, M.; Kitagawa, Y.; Matsuura, Y.; Sato, K.; Suzuki, M. *J. Phys. Chem.* **1996**, *100*, 0, 9138.
(15) Kobayashi, M.; Kaneko, F.; Sato, K.; Suzuki, M. *J. Phys. Chem.* **1986**, *90*, 6371.
(16) Kaneko, F.; Yamazaki, K.; Kobayashi, M.; Kitagawa, Y.; Matsuura, Y.; Sato, K.; Suzuki, M. *Acta Crystallogr.* **1993**, *C49*, *100*, 1232.
(17) Kaneko, F.; Yamazaki, K.; Kitagawa, K.; Takahashi, K.; Kobayashi, M.; Kitagawa, Y.; Matsuura, Y.; Sato, K.; Suzuki, M. *J. Phys. Chem. B.* **1997**, *101*, 1803.
(18) Tasumi, M.; Shimanouchi, T.; Miyazawa, T. *J. Mol. Spectrosc.* **1962**, *9*, 261.
(19) Snyder, R. G. *J. Mol. Spectrosc.* **1960**, *4*, 411.
(20) Snyder, R. G. *J. Mol. Spectrosc.* **1967**, *23*, 224.
(21) Tasumi, M.; Shimanouchi, T.; Watanabe, A.; Goto, R. *Spectrochim. Acta* **1964**, *20*, 629.
(22) Zbinden, R. *Infrared Spectroscopy of High Polymers*; Academic: New York, 1964.
(23) Yano, J.; Kaneko, F.; Kobayashi, M.; Sato, K. *J. Phys. Chem. B* **1997**, *101*, 8112.
(24) Birker, P. J. M. W. L.; Jong, S. D.; Roijers, E. C.; Soest, T. C. V. *J. Am. Oil Chem. Soc.* **1991**, *68*, 895.
(25) Pascher, I. *Curr. Opin. Struct Biol.* **1996**, *6*, 439.

(26) Culot, C.; Norberg, B.; Evrand, G.; Durant, F. *Acta Crystallogr*. **2002**, *B56*, 317.
(27) Dohi, K.; Kaneko, F.; Kawaguchi, T. *J. Cryst. Growth* **2002**, *237*−*239*, 2227.
(28) Chia, N.-C.; Mendelsohn, R. *J. Phys. Chem*. **1992**, *96*, 110543.
(29) Maroncelli, M.; Strauss, H. L.; Snyder, R. G. *J. Chem. Phys.* **1985**, *82*, 2811.
(30) Kim, Y.; Strauss, H. L.; Snyder, R. G. *J. Phys. Chem.* **1989**, *93*, 485.
(31) Yoshii, T. Master thesis, Osaka University, 1999.
(32) Hernqvist, L.; Larsson, K. *Fette. Seifen. Anstrichmittel*. **1982**, 349.
(33) Yano, J.; Kaneko, F.; Kobayashi, M.; Kodali, D. R.; Small, D. M.; Sato, K. *J. Phys. Chem. B* **1997**, *101*, 8120.